Article

Novel Risk Assessment Methodology for Keyhole Neurosurgery with Genetic Algorithm for Trajectory Planning

Iván Villanueva-Naquid [1,*], Carlos Souberville-Montalvo [1], Ruth M. Aguilar-Ponce [2], Saúl Tovar-Arriaga [3], Juan C. Cuevas-Tello [1], Cesar A. Puente-Montejano [1], Marcela Mejia-Carlos [4] and Jaime G. Torres-Corzo [5 6]

[1] Engineering Faculty, Autonomous University of San Luis Potosi, S.L.P., Mexico;
[2] Sciences Faculty, Autonomous University of San Luis Potosi, S.L.P., Mexico;
[3] Engineering Faculty, Autonomous University of Queretaro, S.L.P., Mexico;
[4] Optical Communication Research Institute, Autonomous University of San Luis Potosi, S.L.P., Mexico;
[5] Department of Neurosurgery, Hospital Central "Dr. Ignacio Morones Prieto", S.L.P., Mexico;
[6] Faculty of Medicine, Autonomous University of San Luis Potosi, S.L.P., Mexico;

* Correspondence: ivan.naquid@uaslp.mx; Tel.: +52-444-422-5081

Abstract: Keyhole neurosurgery implies reaching a target area inside the brain through an entry point specified by the neurosurgeon. In order to avoid complications, a risk assessment procedure must be done to establish the minimum risk trajectory from the entry point to the target area. The neurosurgeon establishes the risk values for the brain structure according to the type of intervention. The preset brain structure risk value is used to assess the risk value for each voxel of the brain. This paper proposes an improved risk assessment methodology based on the sum of N maximum risk values for each voxel. Then, risk assessment for a trajectory is done by adding the risk of all voxels that are part of the path. The safest trajectory is defined as the trajectory with the lower risk. Our proposed search trajectory methodology includes a Genetic Algorithm (GA) for finding the safest trajectories. The use of a GA drastically reduces the number of trajectories to analyze, speeding up the planning procedure. The achieved results were qualified by expert neurosurgeons as satisfactory. Our proposed method allows neurosurgeons to calibrate the surgical planning system by allowing them to establish the risk brain structure and the risk value for each structure.

Keywords: genetic algorithms; trajectory planning; keyhole neurosurgery; risk assessment; medical imaging

1. Introduction

One of the main concerns of neurosurgeons in performing brain surgical interventions is to minimize the damage caused during a surgical procedure. The goal of minimally invasive surgery is to operate with a minimum of trauma while achieving maximal surgical efficiency [1]. To increase the success odds in a surgical intervention, a meticulous preoperative planning should be done, in which the determination of multiple factors can be reached such as the best surgical approach point and the safest trajectory to the surgical target. The dimension of the craniotomy is reduced by finding the best surgical approach for an intervention. Therefore, planning surgical trajectories is vital for neurosurgeon. The craniotomy should be as small as possible for minimally invasive exposure but as large as necessary for achieving maximal surgical effect. Therefore, limited exposure is not the primary goal but the result of the keyhole concept, with the main and most important goal being to avoid surgery-related complications [2].

Keyhole neurosurgery is an invasive intervention which attempts to reach a target area in the brain. The definition of the entry point is crucial for the surgical procedure. One key problem in a surgery is planning the trajectory from a surgical approach to the target area. Once the entry point has been selected, the surgical tool should follow a trajectory from it to the target. In keyhole neurosurgery the main goal is to find the best corridor to make a straight trajectory which is easier to perform. A poor decision in the trajectory selection could lead to cause further complications such as bleeding, damage of fundamental cerebral functions or even death [3]. In order to achieve a considerable risk reduction in surgical interventions, the search for incision areas and trajectories with lower risk is a great interest topic for neurosurgeon.

Modern medical imaging techniques have given rise to the development of methodologies for the construction of data analysis systems for medical applications such as lesion segmentation and diseases diagnosis [4]. Such systems use information extracted from medical images datasets obtained by computed tomography (CT) or magnetic resonance imaging (MRI), providing surgeons with tools for better decision-making.

Medical image data is obtained by several methods such as CT and MRI, where a contiguous series of image slices are captured [5]. Each slice denotes a cut through the scanned body structure with a particular thickness. The pixels within each image slice are represented by scalar values that can be interpreted as intensity values [6]. Each slice represents a movement in the z-axis of the 3D image. The minimum processing unit in a 3D image is a volumetric pixel (voxel).

An application of medical imaging techniques is the planning of surgical trajectories, which is an auxiliary tool used by the neurosurgeons in the decision making process for surgical interventions. The problem of planning surgical trajectories can be divided into two stages: assessment of risk values for each considered voxel and search of the minimum risk trajectory. Multiple investigations have been carried out and several techniques have been proposed to calculate the risks in the surgical trajectories using the patient's medical images [7-15].

The interest in surgery trajectory planning has sparkled several methodologies. Vaillant et al. proposed association of risk values to brain structures [7]. Then a risk map of the brain is obtained through Atlases and image registration techniques. This map contains the risk values for each voxel associated to a preset risk of a brain structure. Then a weighted sum of the risks associated with each voxel is calculated to obtain a trajectory. However, this work does not calculate a risk map of the brain and also does not consider the length of the trajectory. Additionally the use of Atlases limits the accuracy of the method since the risk structures were not obtained from the patient images.

Lee et al. proposed an assisted planning trajectory tool based on the combination of patient MRIs with a 3D Brain Atlas [8]. The method is capable of locate risk structures as well as tool insertion point. However, the trajectory is obtained manually by the expert neurosurgeon assisted by the proposed system. This implies a random search for the trajectory with less risk, but does not assure to find the safest trajectories.

The automatic acquisition of trajectories became a point of interest, so in the proposal of Fujii et al. it was presented a work on automatic trajectory planning using the blood vessels as risk structures [9]. The authors proposed a Cost of Blood Vessel Dominant Area (CBVDA) function to calculate risk associated to blood vessels. This function was based on the distance between the voxels of the risk structure and the planned trajectory. Nevertheless, this approach considered as a risk structure only blood vessels. Additionally, the selection of the trajectory was based on analyzing all possible trajectories to find a minimum risk trajectory. The calculation of all possible trajectories leads to a high computational load causing elevated processing times.

The use of trajectory search algorithms extends to different types of brain surgical interventions. Brunenberg et al. proposed a methodology for Automatic Trajectory Planning in Deep Brain Stimulation interventions. In this work, the trajectory risk was calculated based on Euclidean distance between the trajectory and the risk structures [10]. A preset threshold determines the maximum distance allowed to find the best trajectory. Then, all possible trajectories within the threshold were calculated and the minimum risk trajectory was selected. The computational cost was reduced due to the limited number of trajectories. However, if the best trajectory is outside the preset threshold the algorithm will only find a suboptimal trajectory.

Shamir et al. determined risk structures to voxels belonging to brain structures such as blood vessels and ventricles. Then, risk values were associated to each voxel based on the distance to risk structure voxels forming a risk map. A trajectory risk was defined as the weighted sum of the risk value of all voxels that cross the trajectory. Then, all possible trajectories were calculated from the set of entry points to a set of target area. The minimum risk trajectory was selected [11]. However, this definition of the risk trajectory cost does not consider that a voxel is surrounded by two or more brain structures.

Essert et al. used ventricles and sulci segmented from MRI images as a risk structures. Then, marching cubes approach was used to obtain 3D meshes of risk structures. A set of rules indicating the risk conditions in deep brain stimulation (DBS) were defined. Subsequently, the set of rules were divided in soft and strict restrictions. The division was based on the importance of the surgical rule. Then, the optimal trajectory was defined as the lowest risk trajectory based on the rules and restrictions previously defined [12]. However, to estimate the best trajectory, the calculation must be made for each of the candidate trajectories.

The amount of information that must be processed for trajectory planning is large, leading to high processing times. Therefore, a speed up in the algorithm was proposed by Rincon-Nigro et al. [13]. This method employed meshes for grouping multiple voxels information which greatly reduced the amount of information to be processed. In addition, the information was processed using Graphic Processing Unit (GPU) which resulted in short processing times. Although better results were obtained in terms of processing time, the acquisition of the risk map by meshes and not by voxel decreases the precision to the algorithm because close voxels with the same risk are gather into a mesh.

An improvement of the methodology presented by Shamir [11] was introduced by De León-Cuevas [14]. In this work, a fuzzy logic system for trajectory evaluation was proposed. The authors proposed a set of fuzzy rules corresponding to the soft and strict restrictions. Like other works, this proposal requires a thorough calculation of the risk of each trajectory.

Hamze et al. performed a comparison of several methodologies for planning trajectory in deep brain stimulation procedures [15]. This methodology used a model of triangular surface meshes of the sulci, the ventricles and the subthalamic nucleus segmented from MRI images. The neurosurgeon assigned a risk value to each mesh. Then, the risk assessment is done by means of several methodologies to compare the results. In this work, a Non-dominated Sorting Genetic Algorithm II (NSGA-II) was employed, resulting in lower processing time to find the safest trajectory. This algorithm was based on stochastic search of trajectories considering an initial population of N possible trajectories and performing crossover and mutation operations in an iterative stage of M generations. Although processing times were improved by the use of the

NSGA-II algorithm, the accuracy of the risk values decreases due to the calculation of risk in meshes instead of individual voxels.

All previous methodologies are summarized in Table 1. The surgical trajectory planning is basically an optimization problem that tries to find the optimal trajectory that minimize the risk to damage an important brain structure. All previous approaches differ in the definition of risk structures and cost function. However, the processing time is high due to the fact that most of the methodologies performed an exhaustive search of trajectories forcing them to calculate all possible trajectories. In order to speed-up the process, a limited area of search has been proposed. However, this limitation may cause to find a sub-optimal trajectory. Additionally, association of voxels in grids or meshes have been proposed to accelerate the process. However, these approaches suffer from lost in precision. On other hand, the function cost in most cases consider the distance to risk structure but only consider one structure, leading to an unrealistic scenario because more than one structure surrounds each voxel.

Table 1. Comparison of previous approaches in trajectory planning for image guided neurosurgery.

Method	Risk Evaluation	Trajectory Search	Additional Considerations
Vaillant et al. [7]	Weighted sum	Exhaustive search	Atlas Image registration
Lee et al. [8]	No risk evaluation	Manual	Atlas Image registration
Fujii et al. [9]	Maximum	Exhaustive search	Voxel Based
Brunenberg et al. [10]	Maximum	Distance threshold	Atlas Image registration
Shamir et al. [11]	Maximum	Exhaustive search	Voxel based
Essert et al. [12]	Geometric constraints	Rules based solver	Mesh based algorithm
Rincon-Nigro et al. [13]	Avoid critical meshes	Trajectory length	Mesh based algorithm
De León et al. [14]	Maximum	Fuzzy logic	Voxel based
Hamze et al. [15]	Weighted sum	NSGA-II/Montecarlo	Mesh based algorithm
Current approach	Sum of N Maximum	GA	Voxel Based

The proposed methodology allows the configuration of the brain structure that will be considered as risk structures. The selection of the brain structures is done by the end user (neurosurgeon) and depend on the type or surgery that will be performed. This feature gives the neurosurgeon the ability to adapt the calculation of the trajectory taking into account the risks corresponding to the type of intervention as well as the particular case of a patient, obtaining a set of suggestions for the safest trajectories. An improvement over the risk assessment is performed by introducing the value of multiple risk structures that surrounds a given voxel. The risk map is based on the segmented risk structures using patient's information. The accuracy of the results are guarantee by assessing the risk for each voxel instead of using a set of voxels gather in a mesh.

The main objective of this work is the improvement of technical planning of surgical trajectories through a risk assessment that includes multiple structures and the use of optimization algorithms for the searching the minimum risk trajectory. Thus, the contributions of this work are the generation of a risk map that includes more than one structure that surrounds a given voxel and the use of a genetic algorithm (GA) to perform a search of the trajectory with the least risk, without the need to apply an exhaustive search of all the possible trajectories, considering a set of entry points that they draw straight trajectories towards a series of target points. GA provides an adaptive search methodology in complex scenarios [16-19], because GA are known as global search methods avoiding local minima, overcoming typical optimization algorithms. Therefore, they are a viable option to solve the problem of trajectory planning.

The remainder of the paper is organized as follows. Section 2 describes the proposed methodology showing all the operations to be done in the medical image such as brain structures

Preprints (www.preprints.org) | NOT PEER-REVIEWED | Posted: 22 October 2018 doi:10.20944/preprints201810.0464.v1

segmentation (2.1) and the proposed risk assessment methodology (2.2) and selection of trajectories (2.3). Section 3 shows the application of the methodology in a case of study. Conclusions and results are presented in section 4.

2. Materials and Methods

Surgical trajectory planning involves several steps. Figure 1 shows the proposed methodology workflow. The method begins with the medical image dataset under consideration.

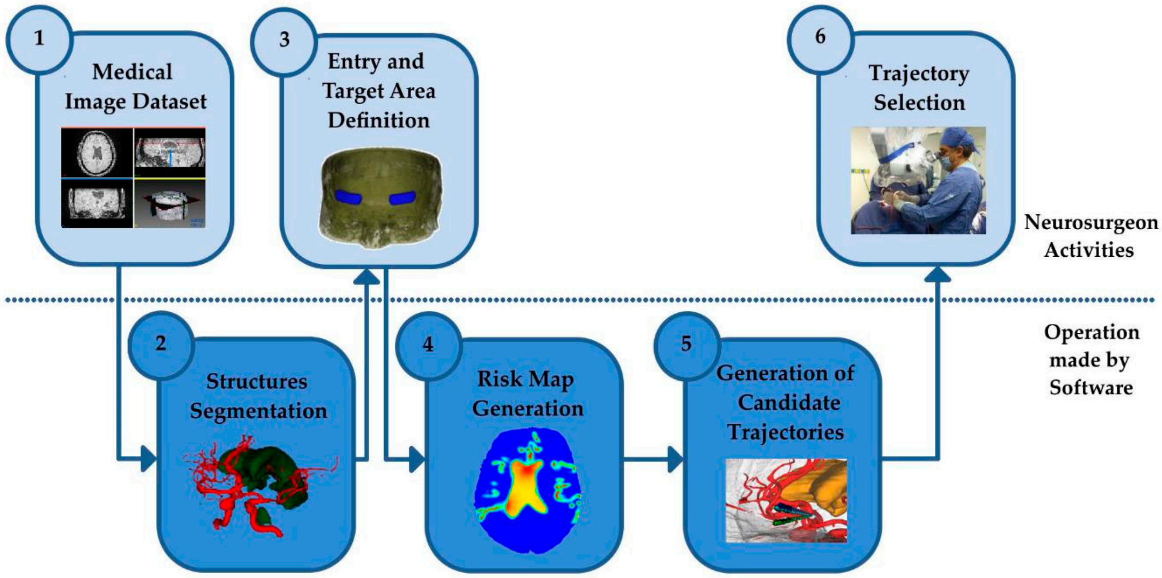

Figure 1. Proposed workflow for trajectory planning.

Once the input data has been selected, segmentation of brain structures is performed. The brain structure considered in this work are cranial surface, cerebral cortex, blood vessels and ventricles. Using the patient's images and the segmented cranial surface the neurosurgeon can select the target area and the entry area respectively. Then, the risk map is calculated using the defined risk structures (blood vessels and ventricles). The candidate trajectories are generated using the risk map. Then the obtained trajectories are shown to the neurosurgeon.

The medical images used in this work are formatted in the Digital Imaging and Communications in Medicine (DICOM) standard with a resolution of N x M voxels. The specific set of images used is a Magnetic Resonance Angiogram (MRA) with a resolution of 512 x 514 and 236 slices each slice has a thickness of 0.51 mm.

2.1. Structures Segmentation.

Segmentation can be defined simply as the partitioning of a dataset into disjoint sets whose member elements have commons and cohesive properties [20]. The segmentation of several structures in the brain was performed using the Medical Imaging Interaction Toolkit (MITK) [21].

The segmentation of the cranial surface is done using thresholding techniques. The principle of the thresholding techniques is based on the correct selection of the appropriate thresholds to divide the pixels of the image and to separate the objects from the background [22]. This operation is expressed by the following equation:

$$S(x,y,z) = \begin{cases} 0 & f(x,y,z) < T \\ 1 & f(x,y,z) \geq T \end{cases}, \quad (1)$$

where $S(x,y,z)$ is the function that indicates the gray level value of the image in the coordinate (x,y,z) and T is the value used as threshold. Usually the selection of the value of T is done manually by verifying the correct segmentation of the objective area. However peaks and valleys of the image histogram can help in choosing the appropriate value for the threshold.

The cranial surface segmentation provides an image where the neurosurgeon can define an entry area that consists of all possible starting points of the candidate trajectories. Segmentation also provide the isolation of the brain to start working in the risk map. This technique is also used to make the brain segmentation.

Structures selected by the neurosurgeon for the calculation of risk are segmented using region growing flood-fill technique [20]. This method begins with a set of seed voxels within the region R. For all voxels connected to the seeds, a similarity function $S(p_1, p_2)$ is applied by means of which the connected voxels that meet this function are added to the region R. If the similarity function is based on a threshold value, it can be expressed by the following equation:

$$S(p_1, p_2) = \begin{cases} 0 & |g(p_1) - g(p_2)| < T \\ 1 & |g(p_1) - g(p_2)| \geq T \end{cases}, \quad (2)$$

where the function $g(p_x)$ returns the gray level value of the voxel p_x and T is the threshold value. If the function S applied to the Voxel seed p_1 with a connected voxel p_2 and it results in the similarity of both voxels, then p_2 is added to the segmented region and becomes a new voxel seed. Equation 2 can be extended with the objective of using two threshold values, one upper and one lower:

$$S(p_1, p_2) = \begin{cases} 0 & |g(p_1) - g(p_2)| > T_{lower} \wedge |g(p_1) - g(p_2)| < T_{upper} \\ 1 & |g(p_1) - g(p_2)| \leq T_{lower} \vee |g(p_1) - g(p_2)| \geq T_{upper} \end{cases}. \quad (3)$$

The segmented images of risk structures obtained, will be used later in the risk labelling process. For this work, the risk structures segmented were the blood vessels and ventricles. Ventricles are interconnected cerebral cavities that create cerebrospinal liquid to maintain intracranial pressure. Therefore, cannot be damaged. Blood vessels distribute blood through the brain and they should be avoided to prevent a cerebral hemorrhage.

2.2. Proposed Risk Assesment Function

Voxel risk assessment procedure must consider the distance to the preset risk structures. This process is known as risk labeling and is performed for all voxels obtained from the segmentation of the brain.

In the labelling process, a risk percentage is associated to each voxel belonging to a preset risk structure. For this work, the voxels corresponding to blood vessels are assigned a risk value of 70% while the ventricles are assigned a risk value of 30%. These percentages values could change considering the type of surgery and must be defined by the expert neurosurgeon.

Risk labelling should generate a map with the risk value for each voxel reflecting the position of the voxel regarding risk structures. Shamir et al. [11] proposed a risk assessment for each voxel as described in Equation 4. The risk for the voxel (x) is calculated by a ratio of each risk structure divided by the distance from the voxel to that particular risk structure. The maximum ratio is assigned as the risk value of the given voxel (x). The α constant is added to avoid division by zero.

$$risk(\bar{x}) = max\left\{\frac{r_k}{dist(\bar{x}, s_k) + \alpha}\right\} \quad (4)$$

The last equation consider only the maximum ratio to a given risk structure. However, each voxel might be surrounded by more than one risk structure. Therefore, the after mentioned equation does not reflect a realistic scenario. An illustration of this situation is presented in Figure 2. The

Preprints (www.preprints.org) | NOT PEER-REVIEWED | Posted: 22 October 2018 doi:10.20944/preprints201810.0464.v1

distance between Voxel 1 and Voxel 2 to the Risk Structure 1 is the same, and assuming that the two risk structures have the same risk value. When the risk value is calculated using Equation 4, the risk value for Voxel 1 and Voxel 2 are equal, although in reality the risk for Voxel 2 should be greater, reaching this voxel implies passing by two nearby structures of risk, while the Voxel 1 only has a nearby structure.

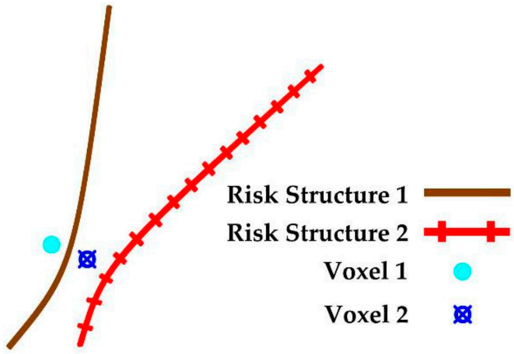

Figure 2. Risk calculation for 2 voxels considering 2 risk structures.

In order to improve the modeling of several risk structure surrounding a given voxel, our proposal is to include *N* maximum values. The value of *N* corresponds to the number of risk structures close to a given voxel.

The set all possible risk values for voxel x with respect to the segmented brain structure is defined in Equation 5.

$$U_x = \left\{ \frac{r_k}{dist(x, s_k) + \alpha} \,\middle|\, 1 \leq k \leq n \right\} \tag{5}$$

The dataset U_x is defined as the risk calculation for the Voxel x regarding to all risk structures s_k. This calculation is made by a division of the risk of the structure r_k and the distance between the structure s_k and the Voxel x. A positive numerical constant α is used to avoid a division by zero. The r_k risk value assigned to each structure s_k only can be assigned by an expert neurosurgeon according to the clinical case. For this study case, the neurosurgeon assigned a risk value of 0.3 to ventricles and 0.7 to blood vessels.

Our proposed approach establishes that the risk value for Voxel x is the sum of k maximum values of the set U_x. Figure 3 shows a block diagram for the calculation of $risk_k$, where k is the number of maximum values to be added.

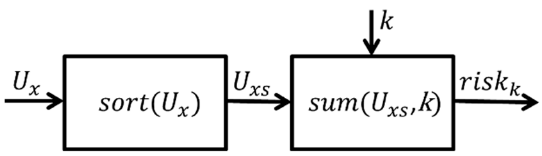

Figure 3. Block diagram of the calculation of risk for k maximum values.

For risk calculation, the U_x values are first sorted downwards, obtaining the U_{xs} array that contains all risk values ordered from higher to lower. Now the sum of the first k values in the U_{xs} array is made, obtaining the value of $risk_k$ equal to the sum of the k maximum values of U_x.

 doi:10.20944/preprints201810.0464.v1

This method is applied to all voxels that are part of the brain (obtained from the brain segmentation), obtaining the risk map as a three-dimensional array that contains the risk values for all the voxels corresponding to that area.

2.3. Proposed Trajectories Selection Algorithm

The trajectory is a set of contiguous voxels that begin in a point of entry and ends in a target area. The trajectory risk is measure as the sum of the voxel risk that compose it. Therefore, this value can be obtained until the risk labelling has been completed. The risk labelling process ends with a risk map that include the risk value for each voxel within the image.

Previous approaches to this problem have searched for the safest trajectory by calculating all possible options and determine the risk associated to each one. Then, the lowest riak value is selected as the safest trajectory. This implies an exhaustive search and thus increases the processing time. Therefore, there is a need to find efficient search mechanism that can find the solution without the need to calculate all possible trajectories.

Searching for a minimum risk trajectory is an optimization problem. GA can be used in these types of problems. These algorithms are designed to mimic the Darwin's fittest principle of survival [23], which is based on the best individuals having a better chance of adapting themselves to a specific environment and surviving, creating an offspring with better genes, which gives them better chances to survive in this environment [24].

The operation of a genetic algorithm consists of the inclusion of a group of individuals who will compete by means of an aptitude function, with the objective of verifying which are the most suitable. The best individuals are reproduced through techniques of crossing and mutation, producing in this way an offspring, which can being reinserted in the population, generating a new population that must produce better results regarding the aptitude function.

GA were proposed by John Holland [17] as means of finding solutions to intractable computationally problems. Since then, this field has grown and is used in a common way in the resolution of optimization problems. The GA is a heuristic search tool widely used for optimization problems, obtained as the composition of selection and mixture (crossover and mutation) that is applied to a population of chromosomes [25]. In this work, the GA was implemented using the Genetic algorithm toolbox developed by A. J. Chipperfield and P. J. Fleming [18]. There are many configurations of a GA, here a single population and elitist strategy is used. It is known as simple genetic algorithm.

GA have been used several times for solving optimization problems in minimally invasive surgery. In 2017, Guo-jun et al employed the non-dominated sorting genetic algorithm II (NSGA-II [26]) to obtain the remote center of motion mechanism for medical robots with better performance indexes and to avoid the collision of multi-manipulators in minimally invasive surgery [27]. The same year, Du et al used the algorithm NSGA-II to carry out a preoperative planning robot-assisted minimally invasive surgery system. In this work was simultaneously optimized the incision placement and the initial pose for the manipulator [28].

Figure 4 illustrates the general operation of the candidate trajectory generation process, where the sets E (entry points region) and G (target points region) are the input for the generation and selection of trajectories process, as a result this process gives all possible trajectories. These trajectories will be processed by the risk calculation process using the risk map to evaluate the risk as the sum of all the voxels that intersects the trajectory. Finally, the trajectories with the least risk will be selected.

 doi:10.20944/preprints201810.0464.v1

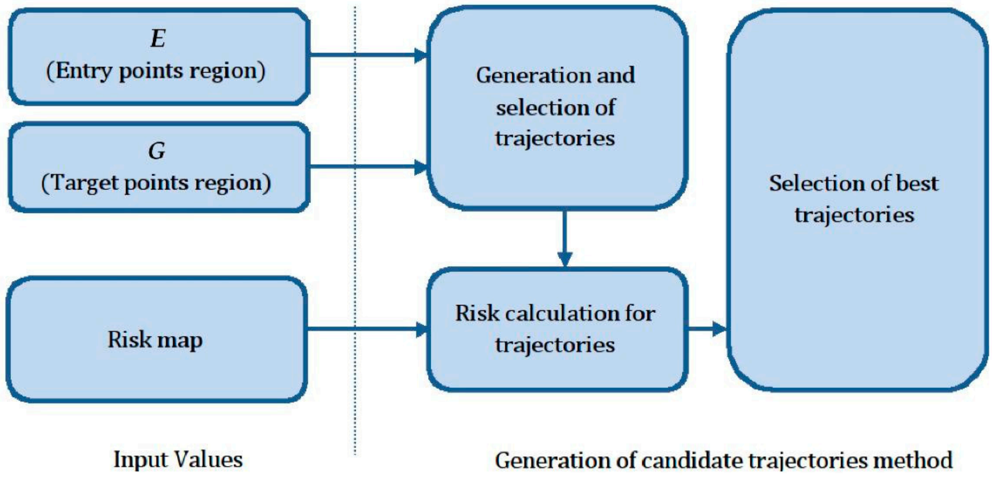

Figure 4. Dataflow for the generation of candidate trajectories.

In the process of generation and selection of trajectories all the possible trajectories are generated by crossing the points in the sets E and G but it is considered a strict constraint corresponding to the distance, in which the trajectories cannot have a length greater than 90 mm. This distance is considered because greater distances to that size can cause damage to the brain tissue [12, 14]. Thus, trajectories that do not fulfill this condition will be eliminated from the selection process.

The population p_x of size k is defined in the following equation:

$$p_x = \left[\begin{array}{cc|c} E_1 & G_1 & f_1 \\ E_2 & G_2 & f_2 \\ \cdots & \cdots & \cdots \\ \cdots & \cdots & \cdots \\ E_k & G_k & f_k \end{array}\right], \quad (5)$$

where each row in p_x is known as a chromosome, which is a set of parameters $\{E_i, G_i\}$, randomly initialized. All the k chromosomes in the population are evaluated using f_i which is the aptitude function. Algorithm 1 shows the proposed aptitude function to evaluate the trajectory.

```
dist ← distance(E_i.x, E_i.y, E_i.z, G_i.x, G_i.y, G_i.z);
if (dist>90)
    f_x ← 100,000,000;
else
{
    f_x ← 0;
    for each voxel v_j that intersects E_i − G_i trajectory
        f_x ← f_x + RiskMap[v_j.x, v_j.y, v_j.z];
}
return f_x;
```

Algorithm 1. Pseudocode for the proposed aptitude function $f_i(E_i, G_i)$ for trajectory evaluation

As can be seen in the proposed aptitude function a pseudo-exaggeratedly high risk (100,000,000) is assigned for distances greater than 90 mm. with the purpose that this trajectory cannot be considered as a viable option by the genetic algorithm.

The complete algorithm that implements the search of the safest trajectory is shown in Algorithm 2.

RiskMap ← Risk calculation for all voxels as shown in section 2.2
Initialize population p_1
Evaluate population p_1 with algorithm shown in Figure 3
for i = 1 to g
{
    Select p_s from p_1
    Recombine p_s
    Mutate p_s
    Evaluate p_s with algorithm shown in Figure 3
    Reinsert p_s into p_1
}

Algorithm 2. Pseudocode for the Genetic Algorithm proposed for candidate trajectories generation.

In this work, the GA was calibrated for use with a population of 800 individuals in a total of 1000 generations with a generation gap of 20%. The selection method used is Stochastic Universal Sampling and the recombination method is a Single Point Crossover. The probability of recombination was calibrated to 70% and the probability of mutation in 10%. For more information about the calibration parameters in a genetic algorithm, please review the documentation for the MATLAB genetic algorithm Toolbox [18].

3. Results

The implementation of the methodology was performed using the MITK Workbench software for segmentation. The GA was implemented using the Genetic algorithm toolbox developed by A. J. Chipperfield and P. J. Fleming [18]. The visualization of structures is done using the Visualization Toolkit (VTK) in C++ programming language [29]. The results obtained by applying the proposed methodology are shown in the next sections.

3.1. Case of Study

The patient images dataset has a resolution of 512 x 414 and comprises a total of 136 slices. The dimension of each pixel in the slices is 0.37 x 0.52 mm. and each slice has a thickness of 0.51 mm. Medical images of the case are shown in Figure 5.

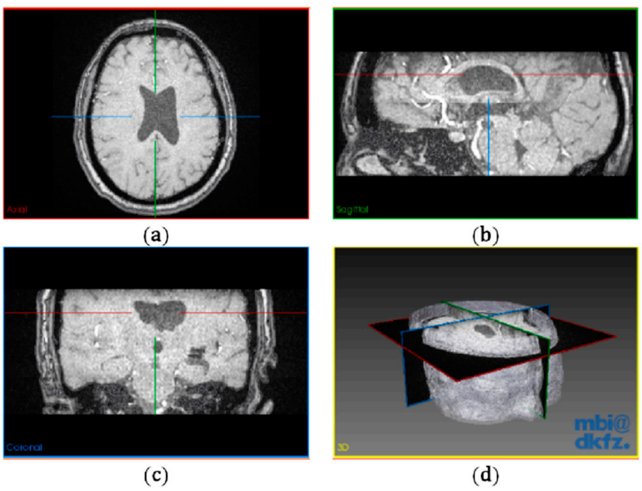

Figure 5. Medical image of the clinical case used as experiment. (**a**) axial view; (**b**) Sagittal View; (**c**) Coronal View; (**d**) Skull reconstruction.

Preprints (www.preprints.org) | NOT PEER-REVIEWED | Posted: 22 October 2018 doi:10.20944/preprints201810.0464.v1

As it could be seen in the proposed methodology, the segmentation is divided into two stages: the segmentation of the cranial surface and the segmentation of the risk structures. The segmentation is done by the neurosurgeon using MITK. The toolkit allows the easy calibration of parameters until the desired segmentation is achieved. This toolkit is widely used in the medical community.

Figure 6 shows the results of applying threshold technique to the dataset. These results were obtained after calibration of two thresholds, the low threshold is considered at a value of 100 while the high threshold is set to a value of 200. Threshold values represent the grey level value that is considered as a limit in the segmentation process.

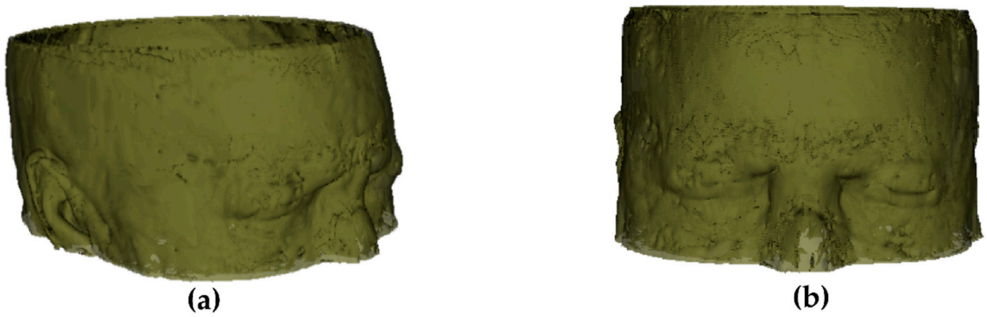

Figure 6. 3D reconstruction of the cranial surface segmentation. (**a**) Lateral View; (**b**) Frontal View;

3.2. Pre-Processing of Input Medical Image

The following step is to determine the risk structures. In this study case, the risk structure selected were the blood vessels and ventricles. The target area is close to these structures.

Blood vessels segmentation was performed using the region growing technique. The seed was placed within one point of the blood vessels and the threshold points were set to 395 for the lower threshold and 1400 for the upper threshold. The result of this process is shown in Figure 7.

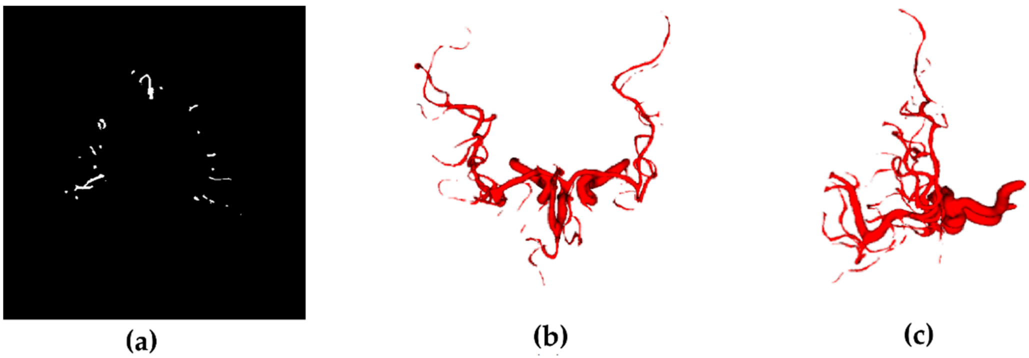

Figure 7. Blood vessels segmentation. (a) Axial slice obtained from segmentation; (b) Top view of the 3D reconstruction; (c) Lateral view of the 3D reconstruction.

Ventricles segmentation is also done by region growing technique. For this purpose the seed is placed within an area of the ventricles and the threshold points are selected with the values of 200 and 240. The result of this process is shown in Figure 8.

Preprints (www.preprints.org) | NOT PEER-REVIEWED | Posted: 22 October 2018 doi:10.20944/preprints201810.0464.v1

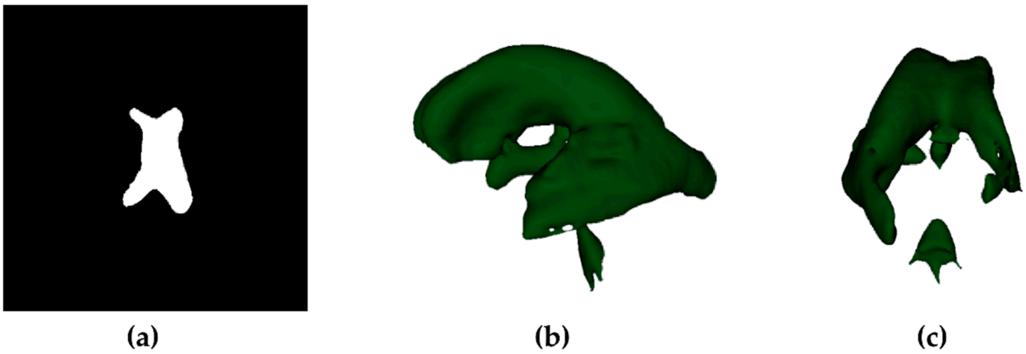

Figure 8. Ventricles segmentation. (a) Axial slice obtained from segmentation; (b) Lateral left view of the 3D reconstruction; (b) Back view of the 3D reconstruction.

The cerebral cortex is segmented in order to get the list of all voxels that must have an assigned risk value. The segmentation is done by region growing with threshold values of 100 and 500.

The 3D reconstruction of all the segmented structures can be seen in Figure 9.

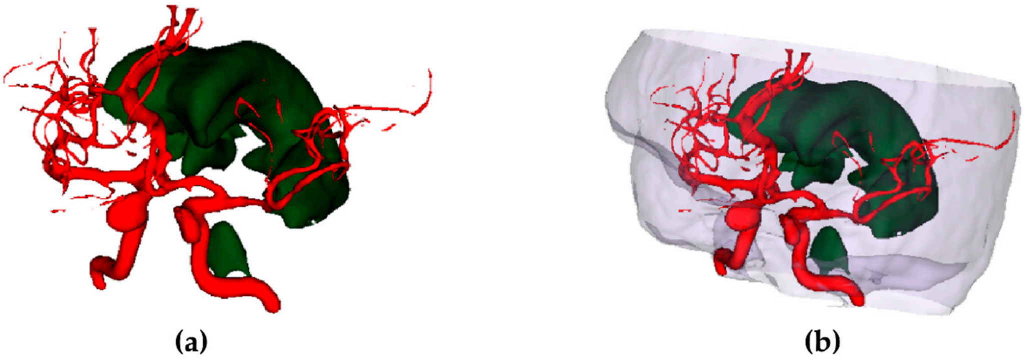

Figure 9. Segmented risk structures. (a) Blood vessels and ventricles; (b) Risk structures and cerebral cortex.

The images that were acquired through these segmentation techniques are a key point in the subsequent calculation of global risk values. Entry point and target area are selected manually by the neurosurgeon using the original image and the segmented images. For this study case, the neurosurgeon selected an area near the supraorbital bilateral keyhole approach [30]. Figure 10 shows the selected entry points as well as the corresponding target area.

Figure 10. Target and entry points. (**a**) Entry points (blue area) and cranial surface; (**b**) Entry points (blue area), target points (yellow area), risk structures and brain cortex.

For this case of study, the target area is very small in which it is necessary to perform an intervention to avoid ruptures of the blood vessels.

3.3. Risk Map Generation

The calculation of the risk map is performed using the segmented structure obtained in the last section. Risk assessment is done for all brain voxels. The set of voxels are obtained by segmentation as was introduced in the last section. Risk assessment is done according to Figure 3. The brain segmentation of the study case in which the tests were applied has a total of 10'595,790 voxels.

The number of maximums *N* to be considered in the calculation is configurable by the expert neurosurgeon, in such a way that it can apply that value according to the type of structures of interest. The proposed methodology establishes that a set of *N* maximum values must be used to determine the specific risk for each voxel. In order to find the best value of *N*, a risk map with *N* equal to 1, 5, 10, and 20 was calculated. A set of slices are shown in Figure 11.

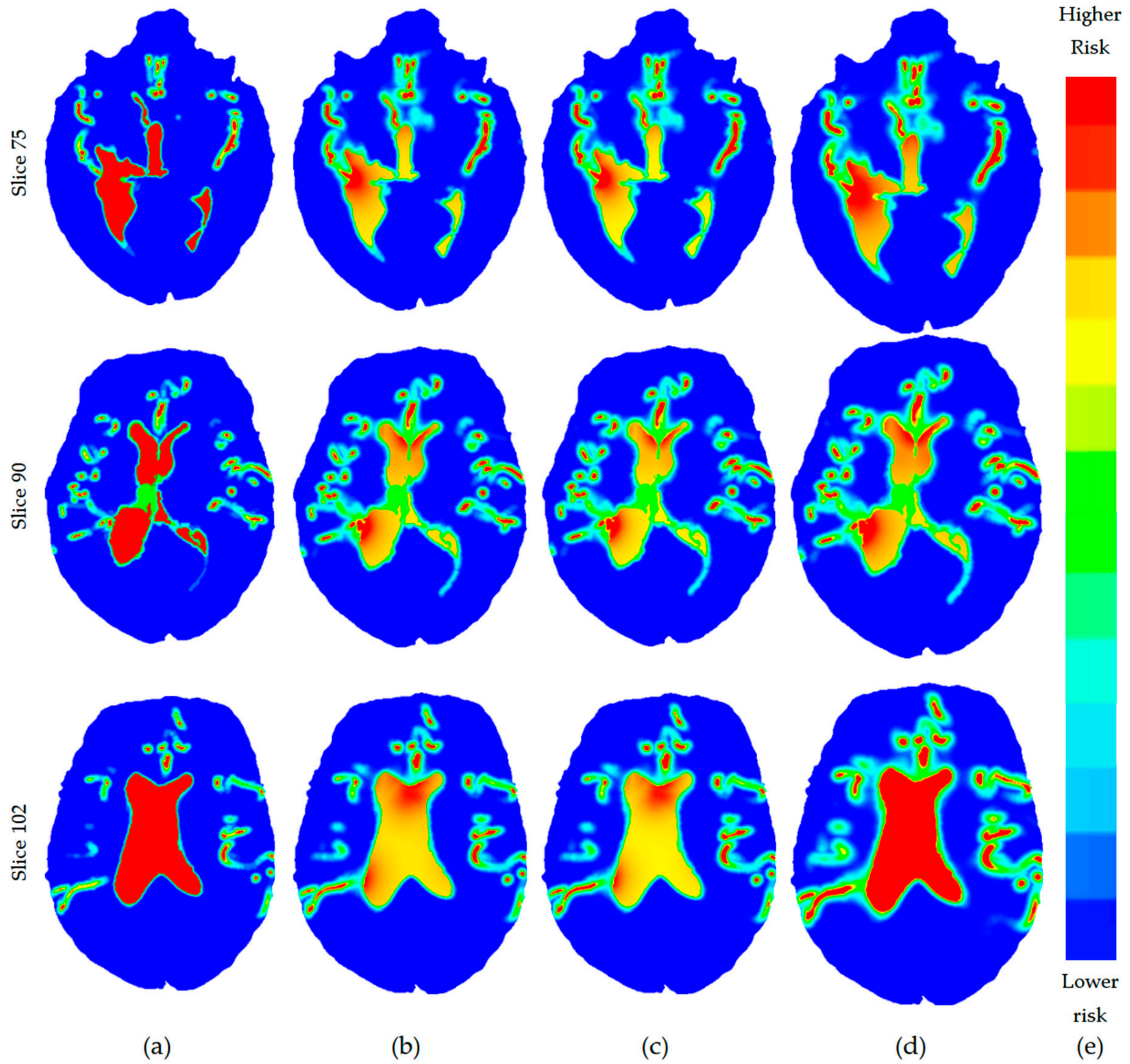

Figure 11. Risk map slices for different values of N. (a) $N = 1$; (b) $N = 5$; (c) $N = 10$; (d) $N = 20$; (e) Risk scale

The color scale of the map's risk is displayed on the right side of Figure 11, being the red color assigned to the greater risk, while blue for the voxels labeled with lower risk

Preprints (www.preprints.org) | NOT PEER-REVIEWED | Posted: 22 October 2018 doi:10.20944/preprints201810.0464.v1

The risk calculation considering only 1 maximum value shows some low-risk vessels and ventricles with a moderate risk. The risk map obtained for 5 maximum values shows an increase in risk when a voxel approaches risk structures. If it approaches blood vessels the risk is greater than the case of ventricles, a situation that shows that blood vessels have priority over the ventricles. The risk maps obtained for N = 5 and N = 10 values are very similar, showing almost imperceptible differences, but the processing time consumed for N = 10 is almost twice the time consumed for the map with N=5. Increasing the N value to 20, the map begins to give preference in terms of risk to the ventricles, giving a lower risk to the blood vessels.

These maps were presented to 5 neurosurgeons to validate which map they consider the best. The unanimous result is that the map of 5 maximum values is the best choice as risk labelling.

3.4. Generation of Candidate Trajectories

The candidate trajectories are calculated using the risk map and the defined entry and target areas. To perform this process a set of points in the entry area must reach another set of points in the target area. In this particular study case there are 11,754,106 possible trajectories, formed by the crossing of all the voxels in the area of entry (57,902 voxels) and the voxels in the target area (203 voxels).

Each trajectory consists of a straight line that passes through all the voxels between the entry (x_1, y_1, z_1) and the target point (x_2, y_2, z_2). So the trajectory T_x is formed by a set of voxels v_i as it is shown in Equation 6

$$T_x = \bigcup_{i=1}^{n} v_i \tag{6}$$

Bressenham's straight line drawing algorithm is used to know all the voxeles that form a trajectory, this algorithm is based on the sum of integer numbers for the acquisition of the next point of the line [31]. As it is shown in Equation 7, the risk of a trajectory R_{T_x} is calculated by the sum of the risks for all the voxeles that form the trajectory.

$$R_{T_x} = \sum_{i=1}^{n} risk(v_i) \tag{7}$$

By applying the algorithms 1 and 2, and considering the calculation of the risk function shown in Equation 7, the safest trajectories are obtained. Figure 12 shows the risks calculation obtained for the trajectories generated with the calibration data mentioned in 2.3.

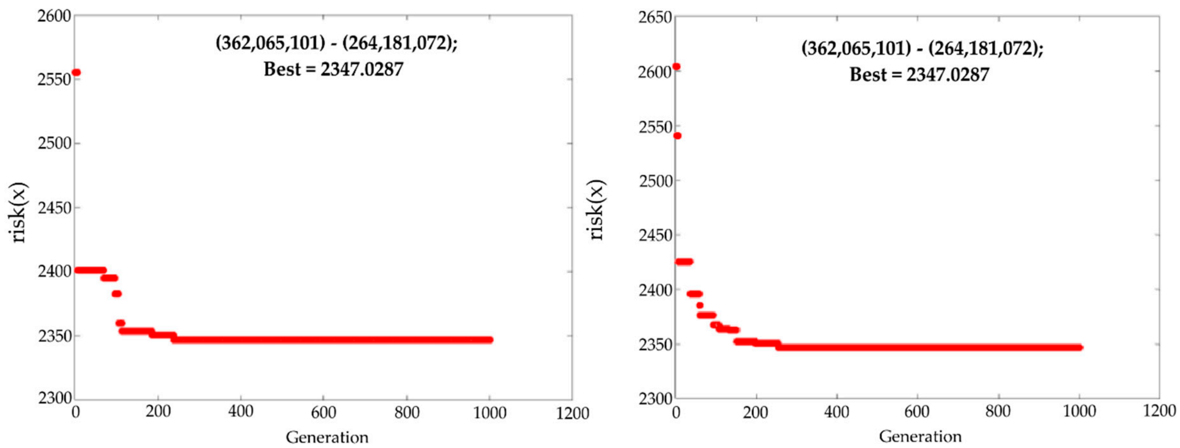

Figure 12. Risk obtained for trajectories by the GA per generation.

In order to test the GA efficiency, an exhaustive calculation of the risks for all the possible trajectories was done. The GA was executed a total of 50 times and the results obtained were

Preprints (www.preprints.org) | NOT PEER-REVIEWED | Posted: 22 October 2018 doi:10.20944/preprints201810.0464.v1

compared with the optimal values obtained in the exhaustive search. With the calibrated parameters, the GA results 42 times in a global minimum and 8 times in a local minimum. By changing the calibration parameters of the genetic algorithm (higher number of population or generations), the incidence of the result corresponding to the global minimum will be greater, as a result, the processing time is also increased. For this study case, the results obtained with these parameters are satisfactory because the 50 trajectories obtained were validated as appropriate by the expert neurosurgeons.

Finally, using VTK, the trajectories obtained are drawn. The trajectories selected by the GA algorithm are shown in Figure 13, where the global minimum is shown in cyan and the two local minimum are shown in blue and green.

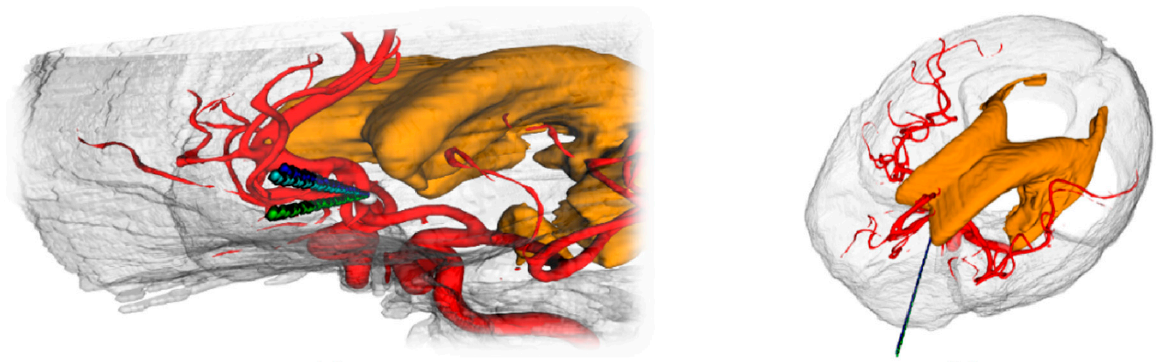

(a) (b)

Figure 13. Candidate trajectories found by the algorithm. (a) Left side view of the trajectories obtained; (b) Top view of the trajectories obtained.

The set of candidates trajectories are shown to the neurosurgeon. The final selection is going to be done by the neurosurgeon. In order to validate the trajectories obtained by our proposed methodology, the trajectories were presented to the neurosurgeon for their evaluation. All the experts agreed that the three trajectories are a good option for this study case.

4. Conclusions and Future Work.

A novel assessment risk methodology for keyhole neurosurgery is presented. The proposed assessment risk function is employed to obtain a risk map. A genetic algorithm is applied to search for the safest trajectory. Segmentation techniques are applied to these images to differentiate several structures such as cranial surface, brain and risk structures (ventricles and blood vessels). With the segmented images the risk assessment process begins and then the search for the safest trajectories is done. In order to get an accurate risk assessment, the proposed risk calculation include several risk structures that surround a voxel. This is accomplished by performing the risk calculation for each voxel as the sum of the N maximum risk values with respect to all risk structures and the distances with the calculated voxel. The risk map shows an allocation of risk values with respect to nearby structures by increasing the value of a voxel when approaching a structure.

The calculation of the risk map using this methodology gave good results and were evaluated visually by a group of neurosurgeons.. Expert neurosurgeons remarks the fact that the map risk values are adequately adapted to the risk values assigned to each structure of interest.

One of the main problems in the search for surgical trajectories is the consumed computation time due to exhaustive searches. Since planning times for surgery are short, the processing time must be minimum. The proposed methodology considers the use of a GA that significantly reduces the processing times in the trajectories search process, avoiding to perform an exhaustive search. Table 2 shows the amount of calculated trajectories and the consumed processing time for both methods: the GA and the exhaustive search. The tests were done on a laptop with

Preprints (www.preprints.org) | NOT PEER-REVIEWED | Posted: 22 October 2018 doi:10.20944/preprints201810.0464.v1

Intel® Core™ i5-3317U processor (up to 2.6 GHz, 3MB L3 Cache) 3rd generation, 4 GB in RAM, 64-bit Ubuntu 18.04.1 operating system.

Table 2. Results comparison of Genetic Algorithm and exhaustive search in applied study case.

Method	Calculated trajectories	Consumed processing time (seconds)
Exhaustive search	11,754,106	103,934.77
Proposed GA	161,000	1,423.63

As can be seen, the processing times using the proposed GA are reduced notably, decreasing a 98.63% the time required to obtain the result.

The results were shown to 5 experienced neurosurgeons. The risk maps obtained for different values of N were showed to them in a blind review. The experts selected the risk map which in his view was the best, coinciding all selections on the map for N = 5. With this risk map, the trajectories search with the GA was done and the results were shown to the 5 neurosurgeons. The trajectories were widely reviewed by the experts, concluding that these trajectories are quite appropriate for the study case.

The proposed methodology provides significant improvements regarding the previous works on the aspect of risk calculation, generating a more complete risk map that considers more risk elements for a voxel. Additionally, the use of a genetic algorithm for candidate trajectories search significantly reduces processing time and the results are more suitable for the neurosurgeons needs.

An opportunity to improve this methodology is to consider additional input information different than the traditional risk structures. The risk concept can be extended to interest areas and brain tracts. Diffusion tensor imaging (DTI) and white matter tractography (WMT) are promising techniques for estimating the course extent, and connectivity patterns of the white matter (WM) structures in the human brain [32]. With the information obtained from a tractography, the neurosurgeon can take radical decisions such as changing the pattern of a surgical approach to preserve tracts displaced or even occasionally make more aggressive approaches when the tracts are already quite destroyed. In the other hand, the inclusion of interest areas require the use of functional Magnetic Resonance Imaging (fMRI), this is mainly used to localize the primary sensory and motor cortex to determine the essential language areas and their hemispheric dominance [33]. The inclusion of the white-matter information (tractography) in conjunction with the cortex information (fMRI) allows the neurosurgeon a more innovative approach for the clinical cases that may arise.

Author Contributions: Conceptualization, Iván Villanueva-Naquid; Formal analysis, Iván Villanueva-Naquid; Investigation, Iván Villanueva-Naquid; Methodology, Iván Villanueva-Naquid, Saúl Tovar-Arriaga and Juan C. Cuevas-Tello; Software, Iván Villanueva-Naquid, Saúl Tovar-Arriaga and Juan C. Cuevas-Tello; Supervision, Carlos Soubervielle-Montalvo and Ruth M. Aguilar-Ponce; Validation, Jaime G. Torres-Corzo; Writing – original draft, Iván Villanueva-Naquid; Writing – review & editing, Carlos Soubervielle-Montalvo, Ruth M. Aguilar-Ponce, Cesar A. Puente-Montejano and Marcela Mejia-Carlos.

Funding: This research received no external funding.

Acknowledgments: Acknowledgments to National Council of Science and Technology (CONACYT) for the support provided to the main author by means of the doctoral scholarship 420956. Acknowledgments are also given to Dr. Jorge G. Reyes Vaca who provided the medical images dataset employed in the work and Dr. Alvín V. de León who gave support in the interpretation of medical images. Thanks to Dr. Mario Alberto Islas Aguilar, Dr. Juan Carlos Chalita Williams and Dr. Roberto Rodriguez Della Vechia for their very valuable opinions used in the validation process.

Conflicts of Interest: The authors declare no conflict of interest

References

1. Perneczky, A.; Reisch, R. Keyhole Approaches in Neurosurgery: Volume 1: Concept and Surgical Technique; Springer Science & Business Media, 2009; ISBN 978-3-211-69501-2.
2. Reisch, R.; Stadie, A.; Kockro, R. A.; Hopf, N. The Keyhole Concept in Neurosurgery. World Neurosurgery 2013, 79, S17.e9-S17.e13, doi:10.1016/j.wneu.2012.02.024.
3. Shamir, R. R.; Joskowicz, L.; Spektor, S.; Shoshan, Y. Localization and registration accuracy in image guided neurosurgery: a clinical study. International Journal of Computer Assisted Radiology and Surgery 2009, 4, 45–52, doi:10.1007/s11548-008-0268-8.
4. Litjens, G.; Kooi, T.; Bejnordi, B. E.; Setio, A. A. A.; Ciompi, F.; Ghafoorian, M.; van der Laak, J. A. W. M.; van Ginneken, B.; Sánchez, C. I. A survey on deep learning in medical image analysis. Medical Image Analysis 2017, 42, 60–88, doi:10.1016/j.media.2017.07.005.
5. Kalavathi, P.; Senthamilselvi, M.; Prasath, V. Review of Computational Methods on Brain Symmetric and Asymmetric Analysis from Neuroimaging Techniques. Technologies 2017, 5, 16, doi:10.3390/technologies5020016
6. Zachow, S.; Zilske, M.; Hege, H.-C. 3D reconstruction of individual anatomy from medical image data: Segmentation and geometry processing. 2007, 13.
7. Vaillant, M.; Davatzikos, C.; Taylor, R. H.; Bryan, R. N. A path-planning algorithm for image-guided neurosurgery. In CVRMed-MRCAS'97; Troccaz, J., Grimson, E., Mösges, R., Eds.; Springer Berlin Heidelberg: Berlin, Heidelberg, 1997; Vol. 1205, pp. 467–476 ISBN 978-3-540-62734-0.
8. Jiann-Der Lee; Chung-Hsien Huang; Shih-Tseng Lee Improving stereotactic surgery using 3-D reconstruction. IEEE Engineering in Medicine and Biology Magazine 2002, 21, 109–116, doi:10.1109/MEMB.2002.1175146.
9. Fujii, T.; Emoto, H.; Sugou, N.; Mito, T.; Shibata, I. Neuropath planner–automatic path searching for neurosurgery. International Congress Series 2003, 1256, 587–596, doi:10.1016/S0531-5131(03)00363-7.
10. Brunenberg, E. J. L.; Vilanova, A.; Visser-Vandewalle, V.; Temel, Y.; Ackermans, L.; Platel, B.; ter Haar Romeny, B. M. Automatic Trajectory Planning for Deep Brain Stimulation: A Feasibility Study. In Medical Image Computing and Computer-Assisted Intervention – MICCAI 2007; Ayache, N., Ourselin, S., Maeder, A., Eds.; Springer Berlin Heidelberg: Berlin, Heidelberg, 2007; Vol. 4791, pp. 584–592 ISBN 978-3-540-75756-6.
11. Shamir, R. R.; Tamir, I.; Dabool, E.; Joskowicz, L.; Shoshan, Y. A Method for Planning Safe Trajectories in Image-Guided Keyhole Neurosurgery. In Medical Image Computing and Computer-Assisted Intervention – MICCAI 2010; Springer Berlin Heidelberg: Berlin, Heidelberg, 2010; Vol. 6363, pp. 457–464 ISBN 978-3-642-15710-3.
12. Essert, C.; Haegelen, C.; Lalys, F.; Abadie, A.; Jannin, P. Automatic computation of electrode trajectories for Deep Brain Stimulation: a hybrid symbolic and numerical approach. International Journal of Computer Assisted Radiology and Surgery 2012, 7, 517–532, doi:10.1007/s11548-011-0651-8.
13. Rincon-Nigro, M.; Navkar, N. V.; Tsekos, N. V.; Zhigang Deng GPU-Accelerated Interactive Visualization and Planning of Neurosurgical Interventions. IEEE Computer Graphics and Applications 2014, 34, 22–31, doi:10.1109/MCG.2013.35.
14. De León-Cuevas, A.; Tovar-Arriaga, S.; González-Gutiérrez, A.; Aceves-Fernández, M. A. Risk map generation for keyhole neurosurgery using fuzzy logic for trajectory evaluation. Neurocomputing 2017, 233, 81–89, doi:10.1016/j.neucom.2016.08.115.
15. Hamze, N.; Collet, P.; Essert, C. Evolutionary approaches for surgical path planning: A quantitative study on Deep Brain Stimulation. In; IEEE, 2017; pp. 1087–1094.
16. Srinivas, M.; Patnaik, L. M. Genetic algorithms: a survey. Computer 1994, 27, 17–26, doi:10.1109/2.294849.
17. Holland, J. H. Adaptation in Natural and Artificial Systems: An Introductory Analysis With Applications to Biology, Control, and Artificial Intelligence; Edición: Reprint.; Bradford Books: Cambridge, Mass, 1992; ISBN 978-0-262-58111-0.
18. Chipperfield, A. J. The MATLAB Genetic Algorithm Toolbox. In IEE Colloquium on Applied Control Techniques Using MATLAB; IEE: London, UK, 1995; Vol. 1995, pp. 10–10.
19. Goldberg, D. E., H., J. H. Genetic Algorithms and Machine Learning. Machine learning 1988, 3, 95–99, doi:10.1023/A:1022602019183.
20. Yoo, T. Insight into Images: Principles and Practice for Segmentation, Registration, and Image Analysis; 1st. edition.; A K Peters/CRC Press: Wellesley, Mass, 2004; ISBN 978-1-56881-217-5.

 doi:10.20944/preprints201810.0464.v1

21. Wolf, I.; Vetter, M.; Wegner, I.; Böttger, T.; Nolden, M.; Schöbinger, M.; Hastenteufel, M.; Kunert, T.; Meinzer, H.-P. The Medical Imaging Interaction Toolkit. Medical Image Analysis 2005, 9, 594–604, doi:10.1016/j.media.2005.04.005.
22. Kang, W.-X.; Yang, Q.-Q.; Liang, R.-P. The Comparative Research on Image Segmentation Algorithms. In 2009 First International Workshop on Education Technology and Computer Science; IEEE: Wuhan, Hubei, China, 2009; pp. 703–707.
23. Shukla, A.; Pandey, H. M.; Mehrotra, D. Comparative review of selection techniques in genetic algorithm. In 2015 International Conference on Futuristic Trends on Computational Analysis and Knowledge Management (ABLAZE); IEEE: Greater Noida, India, 2015; pp. 515–519.
24. Jinghui Zhong; Xiaomin Hu; Jun Zhang; Min Gu Comparison of Performance between Different Selection Strategies on Simple Genetic Algorithms. In; IEEE, 2005; Vol. 2, pp. 1115–1121.
25. McCall, J. Genetic algorithms for modelling and optimisation. Journal of Computational and Applied Mathematics 2005, 184, 205–222, doi:10.1016/j.cam.2004.07.034.
26. Deb, K.; Pratap, A.; Agarwal, S.; Meyarivan, T. A fast and elitist multiobjective genetic algorithm: NSGA-II. IEEE Transactions on Evolutionary Computation 2002, 6, 182–197, doi:10.1109/4235.996017.
27. Niu, G.; Pan, B.; Zhang, F.; Feng, H.; Fu, Y. Multi-optimization of a spherical mechanism for minimally invasive surgery. Journal of Central South University 2017, 24, 1406–1417, doi:10.1007/s11771-017-3545-2.
28. Du, Z.; Wang, W.; Wang, W.; Dong, W. Preoperative planning for a multi-arm robot-assisted minimally invasive surgery system. SIMULATION 2017, 93, 003754971771933, doi:10.1177/0037549717719336.
29. Schroeder, W. J.; Martin, K. M. The Visualization Toolkit. In Visualization Handbook; Elsevier, 2005; pp. 593–614 ISBN 978-0-12-387582-2.
30. Czirják, S.; Nyáry, I.; Futó, J.; Szeifert, G. T. Bilateral supraorbital keyhole approach for multiple aneurysms via superciliary skin incisions. Surgical Neurology 2002, 57, 314–323, doi:10.1016/S0090-3019(02)00698-5.
31. Bresenham, J. E.,Algorithm for computer control of a digital plotter. *IBM Systems Journal*, 4, 25-30, doi: 10.1147/sj.41.0025
32. Chen, X.; Weigel, D.; Ganslandt, O.; Buchfelder, M.; Nimsky, C. Diffusion tensor imaging and white matter tractography in patients with brainstem lesions. Acta Neurochirurgica 2007, 149, 1117–1131, doi:10.1007/s00701-007-1282-2.
33. Tieleman, A.; Deblaere, K.; Van Roost, D.; Van Damme, O.; Achten, E. Preoperative fMRI in tumour surgery. European Radiology 2009, 19, 2523–2534, doi:10.1007/s00330-009-1429-z.